Received: 20 April 2021 | Revised: 22 May 2021 | Accepted: 13 June 2021

DOI: 10.1002/jmor.21386

RESEARCH ARTICLE

JOURNAL OF morphology WILEY

Organization of the central nervous system and innervation of cephalic sensory structures in the water bear *Echiniscus testudo* (Tardigrada: Heterotardigrada) revisited

Vladimir Gross | Lisa Epple | Georg Mayer

Department of Zoology, Institute of Biology, University of Kassel, Kassel, Germany

Correspondence
Vladimir Gross, Department of Zoology, Institute of Biology, University of Kassel, Heinrich-Plett-Straße 40, D-34132 Kassel, Germany.
Email: veegross@gmail.com

Abstract

The tardigrade brain has been the topic of several neuroanatomical studies, as it is key to understanding the evolution of the central nervous systems in Panarthropoda (Tardigrada + Onychophora + Arthropoda). The gross morphology of the brain seems to be well conserved across tardigrades despite often disparate morphologies of their heads and cephalic sensory structures. As such, the general shape of the brain and its major connections to the rest of the central nervous system have been mapped out already by early tardigradologists. Despite subsequent investigations primarily based on transmission electron microscopy or immunohistochemistry, characterization of the different regions of the tardigrade brain has progressed relatively slowly and open questions remain. In an attempt to improve our understanding of different brain regions, we reinvestigated the central nervous system of the heterotardigrade *Echiniscus testudo* using anti-synapsin and anti-acetylated α-tubulin immunohistochemistry in order to visualize the number and position of tracts, commissures, and neuropils. Our data revealed five major synapsin-immunoreactive domains along the body: a large unitary, horseshoe-shaped neuropil in the head and four neuropils in the trunk ganglia, supporting the hypothesis that the dorsal brain is serially homologous with the ventral trunk ganglia. At the same time, the pattern of anti-synapsin and anti-tubulin immunoreactivity differs between the ganglia, adding to the existing evidence that each of the four trunk ganglia is unique in its morphology. Anti-tubulin labeling further revealed two commissures within the central brain neuropil, one of which is forked, and additional sets of extracerebral cephalic commissures associated with the stomodeal nervous system and the ventral cell cluster. Furthermore, our results showing the innervation of each of the cephalic sensilla in *E. testudo* support the homology of subsets of these structures with the sensory fields of eutardigrades.

KEYWORDS
brain, Ecdysozoa, ganglion, Panarthropoda, synapsin, α-tubulin

1 | INTRODUCTION

The composition and segmental nature of the tardigrade brain has been a long-disputed and controversial topic (summarized in Smith & Goldstein, 2017). Part of the controversy stems from our constantly developing understanding of the brain and anterior segments in related groups like arthropods and onychophorans and its broader implications (Martin et al., 2017; Smith et al., 2016; Smith et al., 2018; Telford et al., 2019). Much of the disagreement, however, can be traced to the derived morphology of the anterior nervous system in tardigrades themselves. For example, two pairs of connectives link the brain and first trunk ganglion (compared to only one in arthropods), neural processes are arranged superficially as a ring around the mouthparts giving the appearance of a circumpharyngeal brain, and the number of sensory structures in or on the head often varies between species (e.g., Mayer et al., 2013; Persson et al., 2014; Schulze & Schmidt-Rhaesa, 2013; Zantke et al., 2008). In recent years, a consensus has begun to emerge that the brain represents a single neuromere that may be homologous with the protocerebrum of arthropods and the anteriormost brain region of onychophorans (Gross & Mayer, 2015; Mayer et al., 2013; Smith et al., 2016; Smith et al., 2018). This hypothesis is supported by innervation patterns (Gross & Mayer, 2015; Mayer et al., 2013) as well as expression data from Hox genes and nervous system patterning genes, which suggest more broadly that the entire head is derived from only one segment (Smith et al., 2016; Smith et al., 2018; but see Persson et al., 2012; Persson et al., 2014 for alternative view).

Despite this progress, we still largely lack a more basic understanding of the compartmental composition or substructures and their interconnections that make up the tardigrade brain. This issue has been approached in the past primarily using transmission electron microscopy and immunohistochemistry, but open questions remain (Dewel & Dewel, 1996; Mayer et al., 2013; Persson et al., 2012; Persson et al., 2014; Schulze et al., 2014; Schulze & Schmidt-Rhaesa, 2013; Zantke et al., 2008). It is accepted that the brain consists of several lobes, but do these lobes represent neuromeres? Does the accumulation of nervous tissue in the ventral or ventrolateral part of the brain represent an additional neuromere, such as a subesophageal/subpharyngeal ganglion, or can it be considered as part of the brain itself? Are there additional neuropils within the brain, perhaps associated with the sensory structures or eyes? The cephalic sensory structures in particular, that is, cirri, clavae, papillae, sensory fields, and eyes, often remain to be characterized sufficiently in terms of their function, fine structure, and/or association with the brain proper (Biserova & Kuznetsova, 2012).

In this study, we use an immunohistochemical approach to address these questions by combining a general marker for neurites (directed against acetylated α-tubulin) with a marker for neuropils (directed against the presynaptic protein synapsin) to lay a foundation for understanding the number and relative positions of neuropils within the brain as well as the neural connections between the brain and sensory structures in the head. We use data generated using high-resolution confocal laser scanning microscopy with an Airyscan module to build upon previous investigations and provide a detailed, updated model of the central nervous system and the neurites associated with the cephalic sensory structures in the heterotardigrade *Echiniscus testudo*.

2 | MATERIAL AND METHODS

2.1 | Specimen collection and fixation

Moss and lichen samples were collected from boulders in sunny areas from two locations in Kassel, Germany (51°18′14.3″N, 09°28′08.0″E and 51°17′04.9″N, 09°27′25.0″E) in autumn, 2017. The samples were soaked in tap water in a Petri dish at 21°C and specimens of the heterotardigrade *Echiniscus testudo* (Doyère, 1840) were isolated manually using a glass micropipette. The identity of the species was confirmed based on the redescription by Gąsiorek et al. (2017). The specimens were asphyxiated at 60°C for 30 min and fixed in either 4% formalin in 0.1 mol L^{-1} phosphate-buffered saline (PBS) for 1–2 h for anti-acetylated α-tubulin immunolabeling and scanning electron microscopy, or in a zinc-formalin solution (ZnFA: 18.4 mmol L^{-1} $ZnCl_2$, 135 mmol L^{-1} NaCl, 35 mmol L^{-1} sucrose, 1% formalin in distilled water) for 20 h for anti-synapsin immunolabeling. In both cases, fixation was carried out at room temperature (RT) and animals were punctured during fixation using fine tungsten needles in order to facilitate reagent penetration. Specimens of the eutardigrade *Hypsibius exemplaris* (strain Z151) were kept in laboratory culture, collected, and fixed as described previously (Gross & Mayer, 2019).

2.2 | Scanning electron microscopy

Fixed animals were washed 2 × 15 min in PBS and subsequently dehydrated through an ethanol series (15 min each at 30%, 50%, 70%, 90%, 95%, 100% ethanol). In order to wash away surface contaminants, the animals were then washed for 15 min in acetone, 10 min in xylene, 2 × 15 min again in acetone, and transferred back to absolute ethanol. The samples were then dried using a Bal-Tec 030 critical point dryer (Balzers, Liechtenstein). Dried animals were transferred to double-sided carbon tape on aluminum sample stubs using a fine eyelash hair and sputter-coated with ~30 nm gold–palladium using a Polaron SC7640 sputter coater (Quorum Technologies Ltd.). Imaging was done using a Hitachi S-4000 field emission scanning electron microscope (Hitachi High Technologies Europe GmbH) at an accelerating voltage of 10 kV.

2.3 | Immunohistochemistry

Acetylated α-tubulin is a major component of axons, and therefore an antibody against acetylated α-tubulin was utilized as a general marker for visualizing the overall layout of the nervous system. First, fixed animals were rinsed in PBS and illuminated with bright light of various wavelengths (480, 420–650, 620 nm) for 20 h at 4°C in order to reduce autofluorescence (Neumann & Gabel, 2002). After several washes in

PBS + 1% Triton X-100 (PBS-Tx), the animals were incubated in a mixture of collagenase/dispase (1 mg/ml, Roche Diagnostik GmbH) and hyaluronidase (1 mg/ml, Sigma-Aldrich) for 10–20 min at RT in order to make the nervous tissue more accessible to antibodies. After a 15-min postfixation in 4% formalin at room temperature in order to halt enzyme activity, the samples were washed several times in PBS-Tx and blocked in 10% normal goat serum (NGS, Sigma-Aldrich) for 1 h at room temperature. The samples were subsequently incubated in a solution containing the primary antibody (mouse anti-acetylated α-tubulin, diluted 1:1000; Sigma-Aldrich) + 1% NGS + 0.02% NaN_3 in PBS-Tx for 2–5 days at room temperature. After several washes in PBS-Tx, the samples were incubated in a solution containing the secondary antibody (goat anti-mouse AlexaFluor® 568, diluted 1:500; Invitrogen) + 1% NGS + 0.02% NaN_3 in PBS-Tx for 2–4 days at room temperature. After several washes in PBS-Tx followed by PBS, the samples were counterstained with the nuclear marker SYBR-Green I (diluted 1:10,000 in PBS; Invitrogen) for 30–60 min at room temperature. Finally, the samples were incubated in ProLong® Gold anti-fade mounting medium for at least 2 h, then mounted in the same medium between two glass coverslips and allowed to cure at room temperature for at least 1 day before being sealed with nail polish.

The phosphoprotein synapsin is involved in the release of neurotransmitters at synapses. Markers for synapsin are therefore useful for detecting and visualizing neuropils (Klagges et al., 1996). The following protocol was modified from Ott (2008). Fixed animals were first washed 3 × 15 min in HEPES buffer (10 mmol L^{-1} HEPES, 25 mmol L^{-1} sucrose, 150 mmol L^{-1} NaCl, 5 mmol L^{-1} KCl, 5 mmol L^{-1} $CaCl_2$, pH 7.4). The samples were subsequently incubated in 20% dimethylsulfoxide (DMSO)/80% methanol for 1.5 h, followed by 1 h in 100% methanol, 7 min each in 90%, 70%, 50%, 30%, 0% methanol in 0.1 mol L^{-1} tris-buffered saline (TBS). The specimens were then blocked in 5% NGS in TBS + 1% DMSO (TBS-D) for 1 h, followed by incubation in a solution containing the primary antibody (mouse anti-SYNORF1, diluted 1:100) + 5% NGS in TBS-D for 3 days at room temperature. The monoclonal antibody (mouse anti-SYNORF1, DSHB Product 3C11), deposited by E. Buchner (Klagges et al., 1996) was obtained from the Developmental Studies Hybridoma Bank, created by NICHD of the NIH and maintained at The University of Iowa, Department of Biology, Iowa City, IA 52245. After 3 × 2 h washes in TBS-D, the samples were incubated in a solution containing the secondary antibody (goat anti-mouse AlexaFluor® 568, diluted 1:500; Invitrogen) + 1% NGS in TBS-D for 2 days at room temperature. The samples were then washed 3 × 5 min, 3 × 15 min, 2 × 1 h, and several times over the following 2 days in TBS-D before they were counterstained with SYBR-Green I (diluted 1:10,000 in distilled water) for 1 h. Finally, the samples were rinsed with TBS-D before being mounted in ProLong Gold® as above.

2.4 | Image acquisition and processing

All immunolabeled samples were imaged using a Zeiss LSM880 confocal laser-scanning microscope (CLSM) equipped with an Airyscan module (Carl Zeiss). Image stacks acquired with the Airyscan module were processed using ZEN Blue software with filter strength set to "auto." CLSM substacks were adjusted for contrast and brightness using the Fiji distribution of ImageJ2 (Rueden et al., 2017). Schematics were created and image panels were assembled and labeled using Adobe Illustrator CS5 (Adobe Corporation).

3 | RESULTS

3.1 | Brain

We define the brain of *E. testudo* as the accumulation of nervous tissue in the head belonging to the central nervous system, where the cells and neurites are closely associated with a broad, centrally located, synapsin-rich region (Figures 1, 2, and 3). The brain is roughly horseshoe- or saddle-shaped, lying primarily dorsally and extending laterally (Figures 1 and 2) and occupying much of the space inside the head anterior and dorsal to the pharynx.

The dorsal-most part of the brain is characterized by its innervation of the cephalic sensilla, that is, specifically the internal and lateral cirri, the clavae, and the cephalic papillae, as well as by the prominent, centrally located, synapsin-rich region with low nucleus density (Figures 1, 2, 4, and 5, Video S1). The central brain neuropil is located within this synapsin-rich region, and, while it largely appears as a complex mesh of neuronal connections, we identify two prominent commissures associated with the central brain neuropil, numbered from anterior to posterior (Figures 1 and 3a). Brain commissure 1 is a combination of fibers from the anteriormost part of the brain together with fibers from the inner connectives (Figures 1 and 3a, Video S1). Brain commissure 2 consists primarily of fibers from the inner connectives but may receive neurites from the lateral regions of the brain as well (Figures 1 and 3a, Video S1). In addition, a fork in brain commissure 2 leads to a small and thin dorsal loop within the central brain region (Figures 1 and 3a). An additional, prominent tract is present posterior to brain commissure 2 and consists of a combination of fibers from the outer connectives and the extracerebral outer clusters (Figures 1 and 3a). This posterior nerve tract is similar in morphology to the two brain commissures but is different in that it does not cross the midline, its fibers instead forming a diffuse network around the posterior midline of the central brain neuropil (Figures 1 and 3a). The region posterior to the central brain neuropil consists largely of neuronal somata with little acetylated α-tubulin immunoreactivity (Figures 1 and 2a).

The brain is connected to the first trunk ganglion via two pairs of connectives: the inner and outer connectives (Figures 1, 3c, and 6e). While the inner connectives can be followed unambiguously along their entire length from the first trunk ganglion to the brain commissures, a portion of their neurites are also associated with the extracerebral ventrolateral clusters (Figures 1 and 3c). The outer connectives run along the body wall directly between the first trunk ganglion and the brain, where they enter the latter at its posterolateral margin (Figures 1a and 3c).

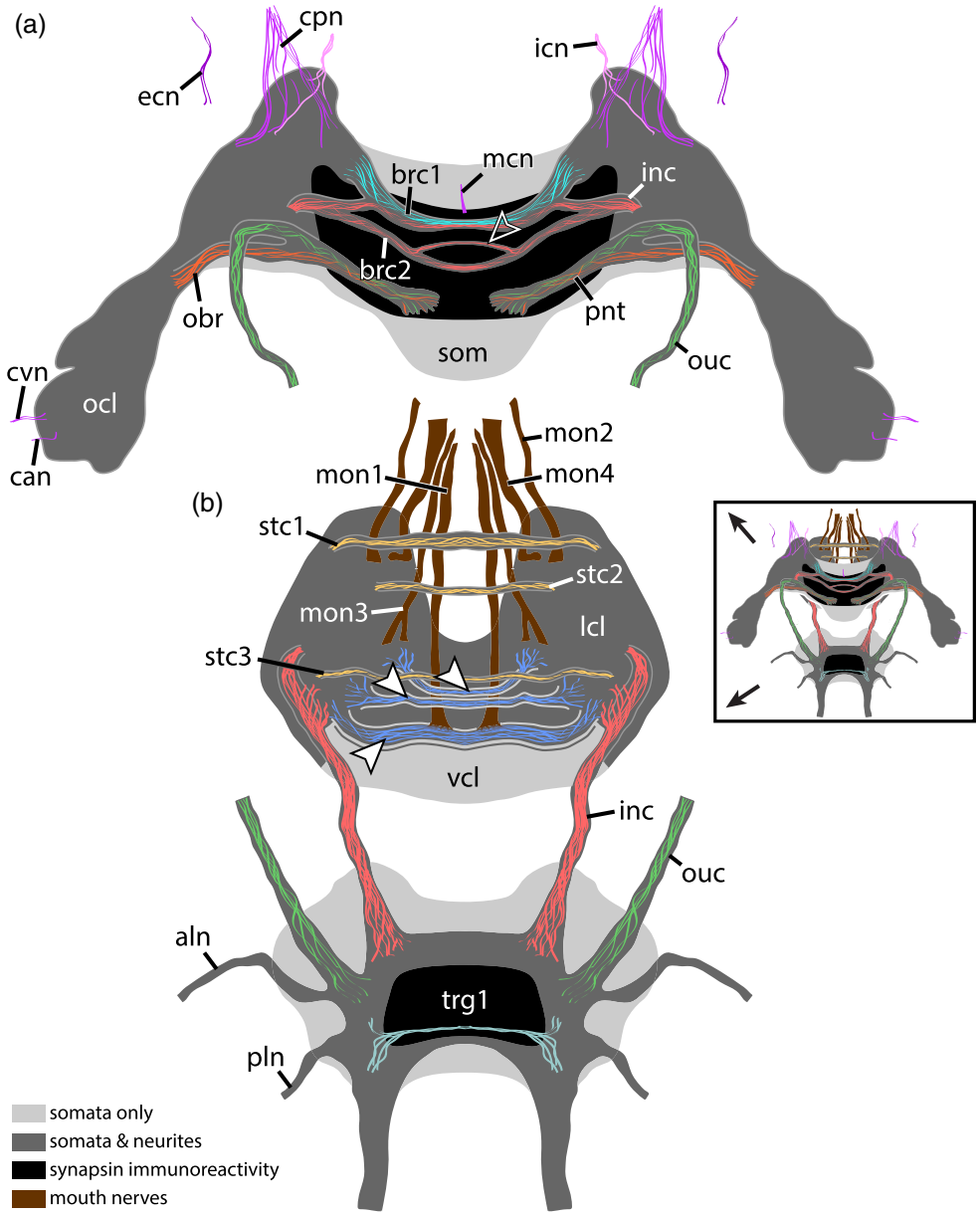

FIGURE 1 *Echiniscus testudo*, nervous system of the head and first trunk ganglion. Simplified diagrams based on nuclear labeling and anti-acetylated α-tubulin and anti-synapsin immunoreactivity. All fibers are shown schematically and do not reflect the real number of fibers present. Anterior is up in both images. Diagrams are not to scale. (a) Major regions of the dorsal brain as well as fibers of the brain commissures, cephalic sensilla, and other tracts. View from ventral. Note that the outer cluster is also shown due to its close association with the brain even though it represents a spatially separate structure. The inner connectives are shown only from their point of entry into the brain. The neurites of the external cirrus lie outside the brain proper. Hollow arrowhead indicates the fork of brain commissure 2. (b) Major regions as well as the fibers of the major commissures and connectives of the central nervous system in the ventral part of the head and first trunk segment. View from dorsal. The inner connectives are shown only up to their point of entry into the ventrolateral cluster. Arrowheads indicate ventral commissures 1–3, from anterior to posterior. Inset shows a combined diagram illustrating the spatial relationship between (a) and (b). aln, anterior leg nerve; brc1–brc2, brain commissures 1–2; can, neurites of cirrus A; cpn, neurites of cephalic papilla; cvn, neurites of the clava; ecn, neurites of external cirrus; icn, neurites of internal cirrus; inc, inner connective; lcl, ventrolateral cluster; mcn, neurites corresponding to median cirrus; mon1–4, mouth nerves 1–4; obr, neurite bridge between brain and outer cluster; ocl, outer cluster; ouc, outer connective; pln, posterior leg nerve; pnt, posterior nerve tract; som, posterior perikaryal region; stc1–stc3, stomodeal commissures 1–3; trg1, trunk ganglion 1; vcl, ventral cluster

3.2 | Extracerebral nervous structures in the head

The ventral side of the head is occupied by an accumulation of nervous tissue but lies outside what we define as the brain (Figures 1b and 3c). The bulk of this nervous tissue is represented by the ventrolateral clusters: bilaterally symmetric regions containing both neuronal somata and neurites (Figures 1b and 3c). The ventrolateral clusters are associated laterally with the inner connectives, which enter the

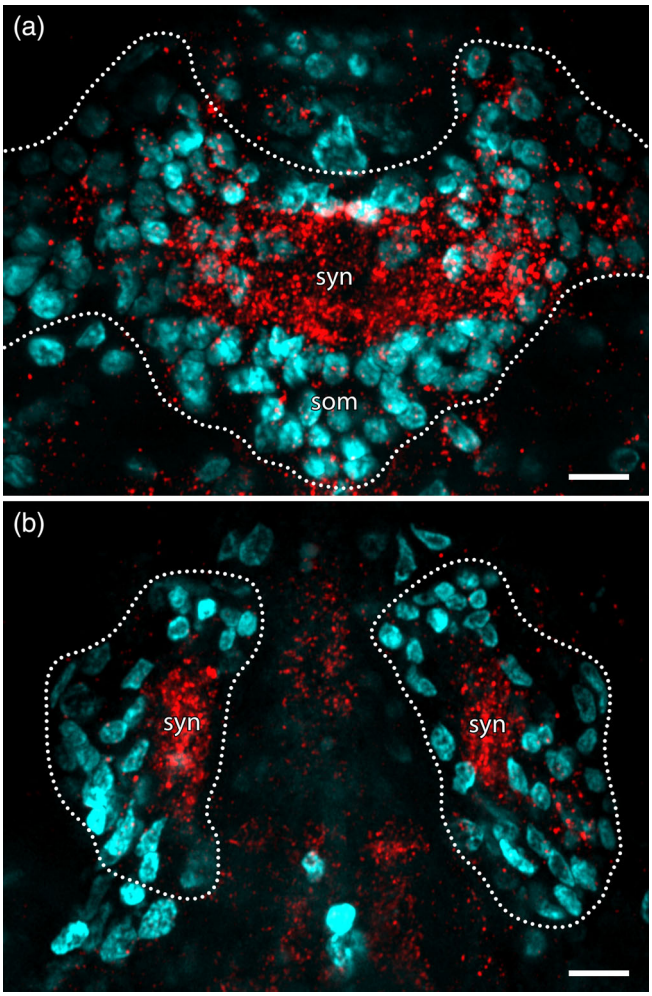

FIGURE 2 *Echiniscus testudo*, synapsin immunoreactivity in the brain. Maximum intensity projections of CLSM substacks showing anti-synapsin immunolabeling (red) and nuclear counterstain (cyan). Dorsal view; anterior is up in both images. Dotted lines indicate the outlines of the brain. (a) Dorsal part of the saddle-shaped brain. The centrally located synapsin-rich region, corresponding to the central brain neuropil, shows relatively few nuclei. A somata-rich region located posteriorly in the brain shows little or no synapsin immunoreactivity. (b) Lateral part of the brain. Substack showing the region immediately ventral to (a), approximately halfway along the dorsoventral body axis. The synapsin signal extends laterally from the central brain neuropil, forming a horseshoe-shaped domain in the head. som, perikaryal region; syn, synapsin-immunoreactive region. Scale bars: 5 μm (in both images)

ventrolateral clusters at their posterolateral borders (Figures 1b and 3c). Different from the brain, the middle region on the ventral side, that is, the ventral cluster, lacks a synapsin signal, and shows a nucleus density comparable to surrounding nervous tissue, for example, the ventrolateral clusters (Figures 1b and 3c, Figure S1). We describe three prominent commissures within the ventral cluster, numbered 1–3 from anterior to posterior (Figures 1b, 3c, and 7a,b). Ventral commissure 1 is the shortest of the three ventral commissures and may be closely associated with nerves innervating the mouth (Figures 3c, 6, and 8b). Ventral commissure 2 fans out laterally into the bulk of each ventrolateral cluster (Figures 1b and 3c). Ventral commissure 3 is associated with the ventral-most mouth nerves medially and meets the inner connectives at the posterior of the ventrolateral clusters laterally (Figures 1b, 3c and 7a). Similar to the dorsal side, the region posterior to ventral commissure 3 of the ventral cluster consists of somata with little or no acetylated α-tubulin immunoreactivity (Figures 1b and 3c).

Three additional commissures, lying approximately halfway along the dorsoventral axis, are associated with the stomodeal nervous system (Figures 1b and 3b, Video S1). These commissures are numbered 1–3 from anterior to posterior. Stomodeal commissure 1 spans the anteriormost region of the ventrolateral clusters while stomodeal commissure 2 links approximately their middle region (Figures 1b and 3b). Stomodeal commissure 3 lies directly dorsal to ventral commissure 1 (Figures 1b, 3b). All three stomodeal commissures are preoral, that is, dorsal to the buccal tube, but according to our data, they are associated neither with the synapsin-rich region nor the brain commissures (Figures 1b and 3a,b).

3.3 | Cephalic sensilla

A total of five pairs of cephalic sensilla (commonly referred to as cephalic sensory appendages) are present in *E. testudo* (Figures 4, 5, and 8). The three frontal cephalic sensilla, that is, the cephalic papillae and the internal and external cirri, are positioned laterally around the mouth cone (Figures 4a, 5a, and 8a). The internal cirri and cephalic papillae are innervated directly by neurons lying within the brain, specifically in the anterior region on the dorsal side (Figure 4e). The exact number of neurites associated with each of these structures is unclear, but the cephalic papilla is clearly more extensively innervated than either the internal or external cirrus (Figure 4d,e). Neurite bundles of the cephalic papilla bifurcate, with one group running toward the midline and possibly contributing to brain commissure 1 while the other set runs to the lateral region of the brain (Figures 1a, 3b, and 4d,e). Similar to the internal cirrus, neurites of the external cirrus are short and associated with one or two neurons that, different from those of the internal cirrus, lie directly under the body wall, outside the brain (Figure 4d). In all cases, neurites terminate at the bases of the cephalic sensilla or, at most, within a short distance proximally inside the structure (Figures 4d,e and 5b–e). The majority of the length of each cephalic sensillum does not exhibit acetylated α-tubulin immunoreactivity (Figure 5b).

Unlike the frontal cephalic sensilla, the clava and cirrus A are found dorsolaterally around the posterior margin of the head, at the front of the scapular plate (Figures 5a and 8a,b). These two structures are innervated by the outer cluster: a local accumulation of neurons that is spatially separated from the central brain but still maintains a direct connection to the lateral region of the brain, where it joins the fibers of the outer connectives (Figures 1a and 5b–e). Combined nuclear and anti-acetylated α-tubulin labeling indicates that this cluster consists of ~17 cells arranged in two lobes: a smaller, anterior lobe with ~5 cells, and a larger, posterior lobe with ~12 cells (Figure 5b,c). From this cluster, two neurite bundles are associated with the clava while one neurite

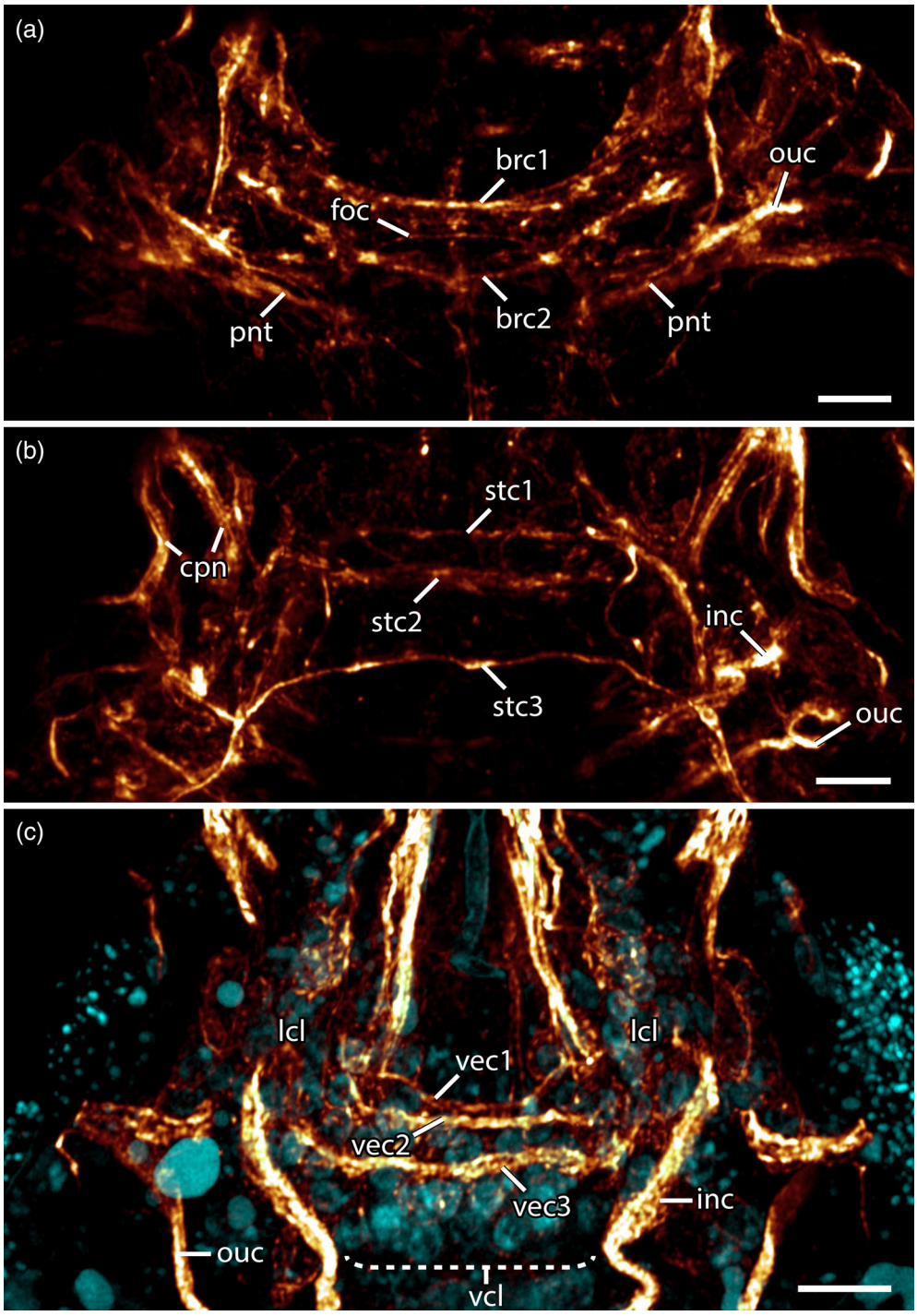

FIGURE 3 *Echiniscus testudo*, commissures and other tracts in the head. Maximum intensity projections of CLSM substacks showing anti-acetylated α-tubulin immunoreactivity (glow) and nuclear counterstain (cyan in c). Dorsal views; anterior is up in all images. (a) Middle region of the brain showing the two brain commissures. Notice the fork in the second brain commissure. The posterior nerve tract is a fusion of neurites of the outer connectives and outer clusters. (b) Region approximately halfway along the dorsoventral body axis showing the three stomodeal commissures. (c) Ventral region of the head showing the three ventral commissures as well as the ventral and ventrolateral clusters. brc1–brc2, brain commissures 1–2; cpn, neurites of the cephalic papilla; foc, fork of brain commissure 2; inc, inner connective; lcl, ventrolateral clusters; ouc, outer connective; pnt, posterior nerve tract; stc1–stc3, stomodeal commissures 1–3; vcl, ventral cluster; vec1–vec3, ventral commissures 1–3. Scale bars: 5 μm (in all images)

bundle is associated with the cirrus A; each neurite bundle terminates at the base of its respective sensillum (Figure 5b–e). Of the two neurite bundles associated with the clava, one enters the anterior lobe and one enters the posterior lobe (Figure 5b,e). The single neurite bundle associated with the cirrus A enters the posterior lobe (Figure 5b,e).

In addition to the well-developed cephalic sensilla described above, we detected a structure corresponding in position to the unpaired median cirrus typical of arthrotardigrades (Figures 4a–c and 8a). Scanning electron microscopy revealed a spot on the cuticle at this position with a higher secondary electron signal and a small pore in its center, clearly distinguishing it from the surrounding cuticular surface (Figure 4a,c). Immunolabeling against acetylated α-tubulin shows that this sensory field is innervated by a single small neurite or neurite bundle in the anterior region of the dorsal midline of the brain (Figure 4b).

3.4 | Mouth nerves

Immunolabeling against acetylated α-tubulin revealed the presence of four double pairs of nerves innervating the mouth cone—located

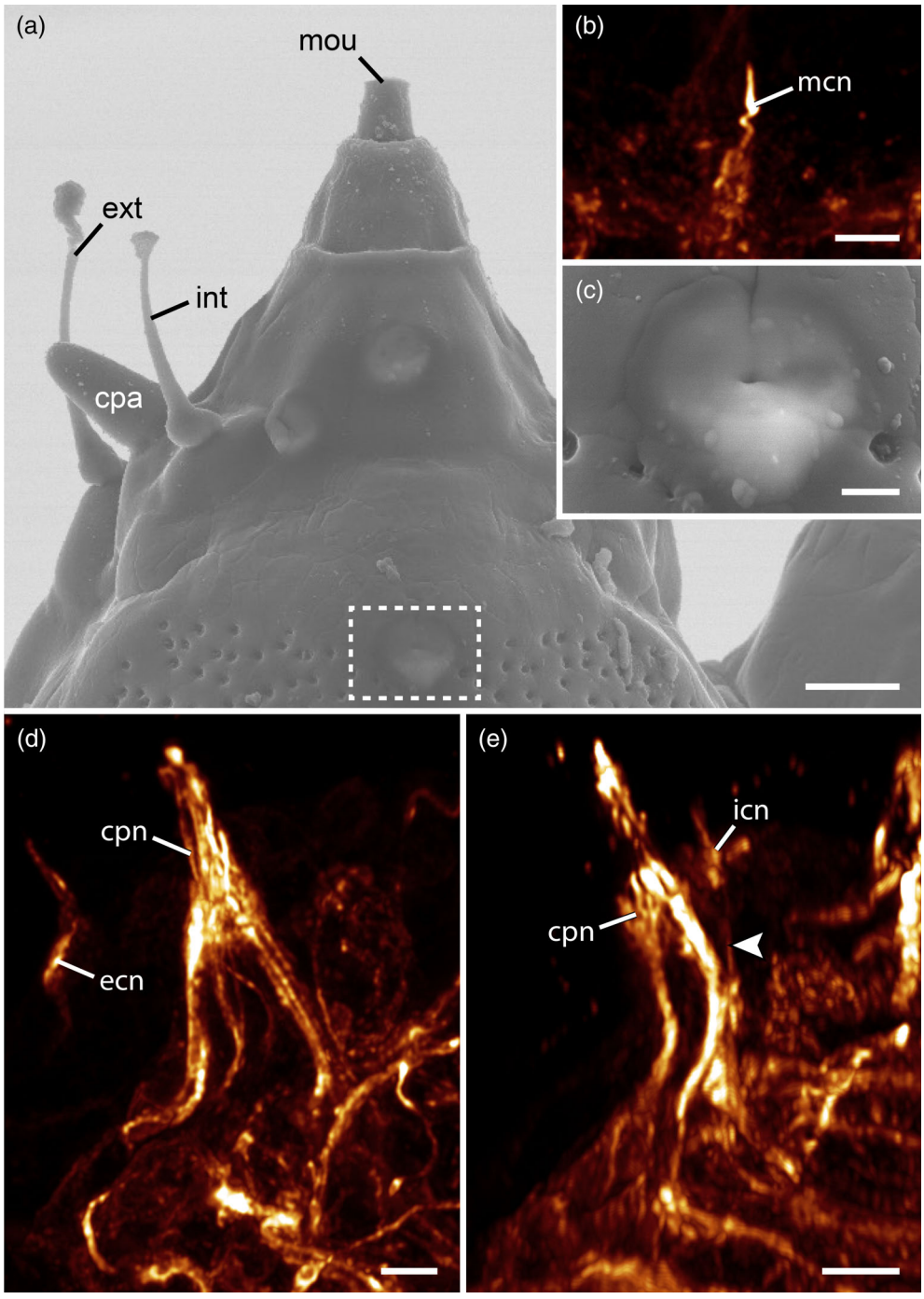

FIGURE 4 *Echiniscus testudo*, anterior cephalic sensilla and their innervation. Scanning electron micrographs (a, c) and maximum intensity projections of CLSM substacks (b, d, e) showing anti-acetylated α-tubulin immunoreactivity. Dorsal views; anterior is up in all images. (a) Three of the five pairs of cephalic sensilla are found in an anterior position, arranged laterally around the mouth cone. A differentiated spot with a small pore in the cuticle of the dorsal head (boxed region) may correspond to the median cirrus of arthrotardigrades. (b) Closeup of the boxed region in (a), where anti-acetylated α-tubulin immunoreactivity reveals a neurite under the spot corresponding to the arthrotardigrade median cirrus. (c) High magnification scanning electron micrograph of the boxed region in (a). (d) Anterolateral region of the left side of the brain showing the innervation of the cephalic papilla and external cirrus. Notice the prominent bifurcation of the neurites of the cephalic papilla. The neurites of the external cirrus are not associated with the brain. (e) Anterolateral region of the left side of the brain but further dorsal compared to (d), showing the innervation of the cephalic papilla and internal cirrus. Arrowhead indicates the neurite of the internal cirrus, running alongside the neurites of the cephalic papilla. cpa, cephalic papilla; cpn, neurites of the cephalic papilla; ecn, neurites of the external cirrus; ext, external cirrus; icn, neurites of the internal cirrus; int, internal cirrus; mcn, neurites of structure corresponding to median cirrus of arthrotardigrades; mou, mouth. Scale bars: a, 5 μm; b, d, e, 3 μm; c, 1 μm

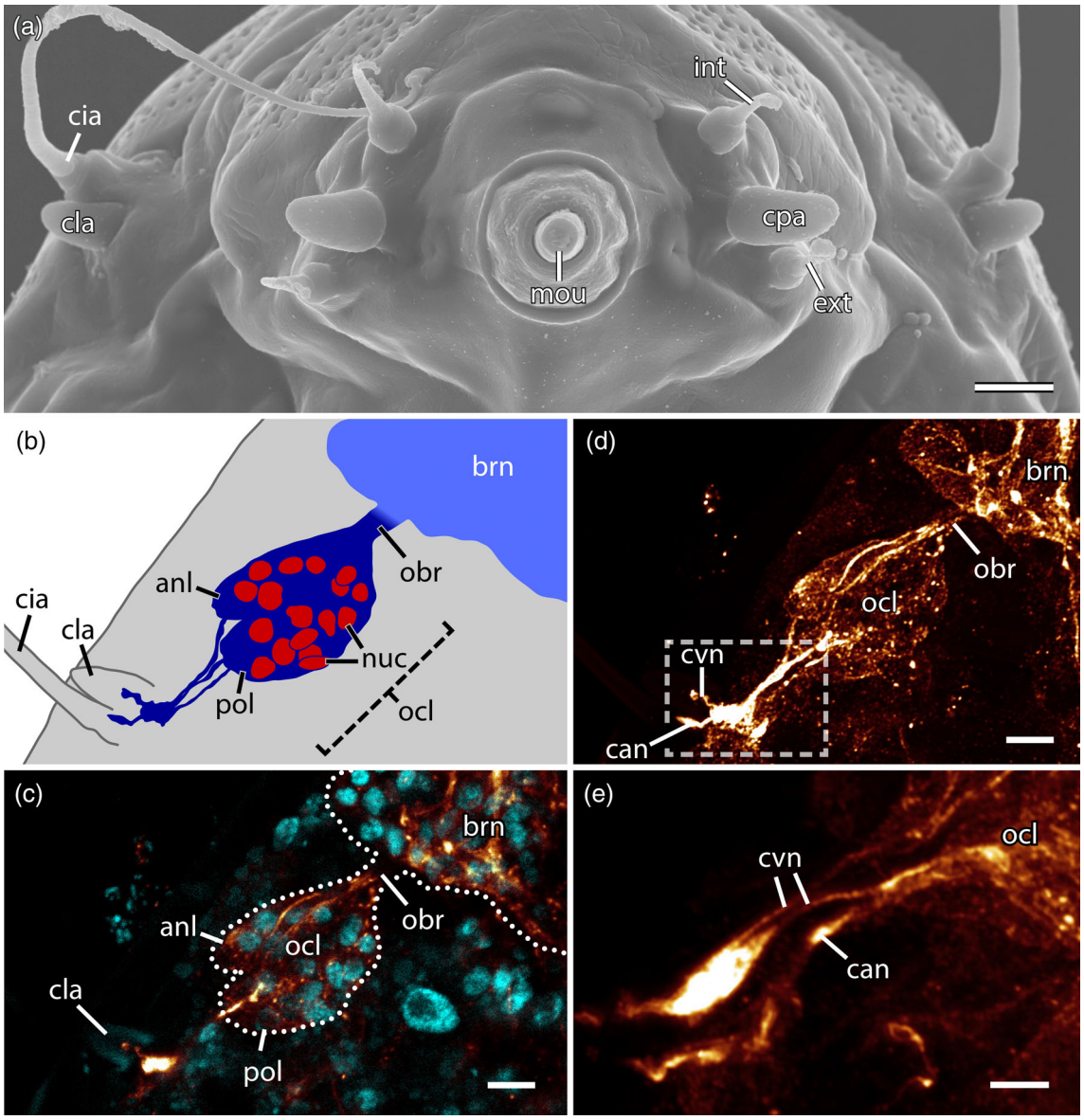

FIGURE 5 *Echiniscus testudo*, outer cluster and innervation of the clava and cirrus A. Scanning electron micrograph (a), schematic diagram (b), and maximum intensity projections of CLSM substacks showing anti-acetylated α-tubulin immunoreactivity (glow in c–e) and nuclear counterstain (cyan in c). (a) Frontal view of the head of *E. testudo* (dorsal is up) showing the five pairs of cephalic sensory structures. Note that the clava and cirrus A are found further posteriorly on the head compared to the three anterior cephalic sensory structures. (b–e) Dorsal views of the left side of the posterior head region; anterior is up in all images. (b) The outer cluster consists of an anterior lobe of ~5 cells and a posterior lobe of ~12 cells and is directly connected to the brain via a narrow bridge of neurites. Neurites from the outer cluster innervate the clava and cirrus A. (c) Combined nuclear and anti-acetylated α-tubulin immunoreactivity showing the composition of the outer cluster. The cuticular part of the clava is autofluorescent. (d) Same region as in (c). Increasing the brightness of the anti-acetylated α-tubulin signal shows the neurites of the outer cluster innervating the clava and cirrus A. (e) Scan of a different specimen showing a closeup of the boxed region in (d). Two neurites innervate the clava and one neurite innervates the cirrus A. anl, anterior lobe of outer cluster; brn, brain; can, neurite of cirrus A; cbr, neurite bridge between the brain and outer cluster; cia, cirrus A; cla, clava; cpa, cephalic papilla; cvn, neurites of clava; ext, external cirrus; int, internal cirrus; mou, mouth; nuc, nuclei; obr, outer cluster neurite bridge; ocl, outer cluster; pol, posterior lobe of outer cluster. Scale bars: a, c, d, 5 μm; e, 3 μm

ventrally or laterally but not dorsally in the head—numbered 1–4 from ventral to dorsal (Figures 1 and 7a–c). The two neurites of each double pair tend to lie close to each other near their anterior ends but are individually distinguishable further posteriorly (Figure 7a–c). Mouth nerves 1 meet ventral commissure 3 within the ventral cluster on either side of the ventral midline, with their somata also likely located around this point (Figure 7a). Mouth nerves 2 come from the anteriormost region of the ventrolateral clusters (Figure 7b). Mouth nerves 3 come from the same region where ventral commissure 1 fans out into the ventrolateral clusters (Figure 7b). Mouth nerves 4 show a similar arrangement to mouth nerves 2 but lie further dorsally and slightly medially (Figure 7c). The anterior ends of each of the mouth

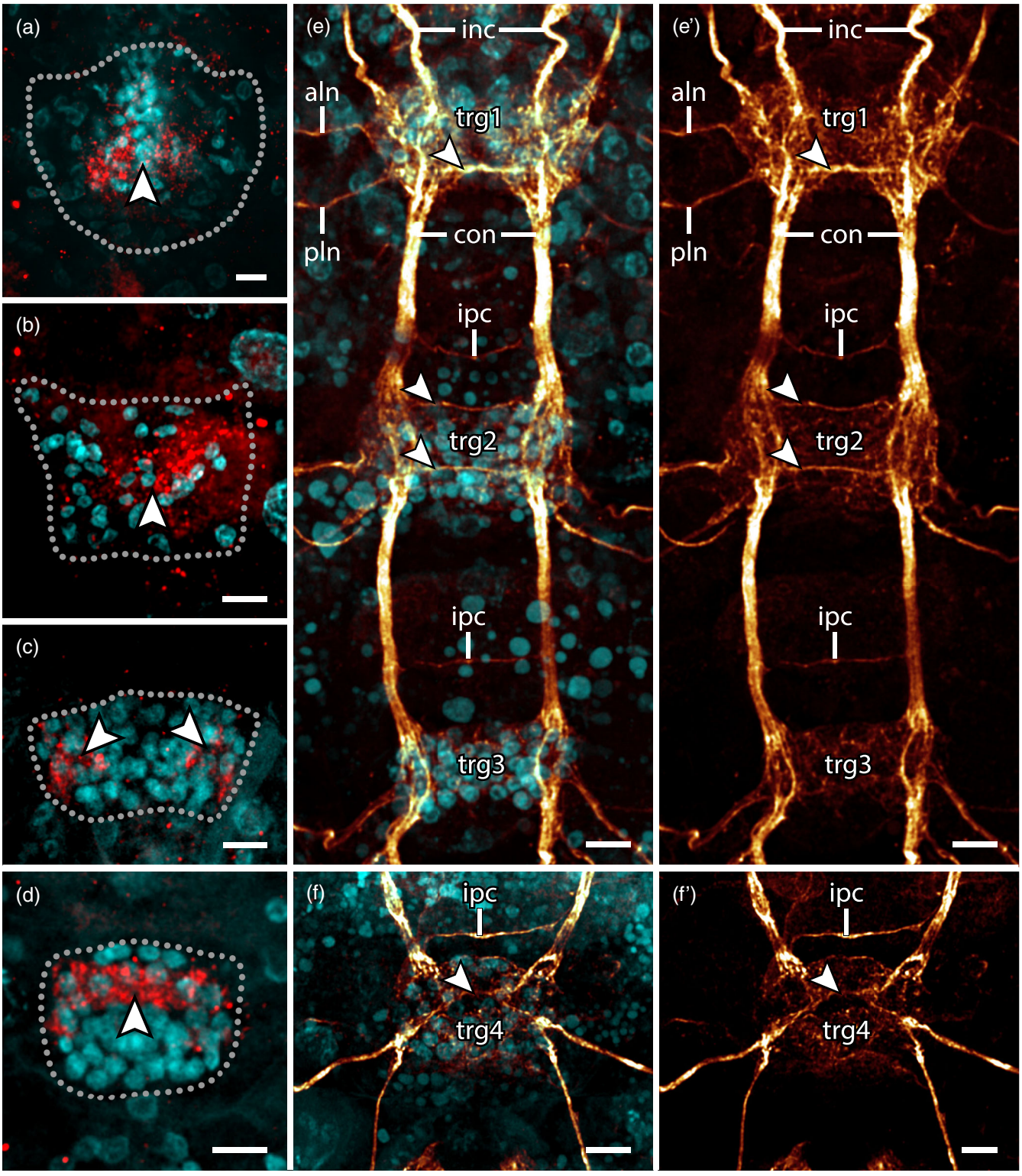

FIGURE 6 *Echiniscus testudo*, organization of trunk ganglia. Maximum intensity projections of CLSM substacks showing anti-synapsin immunoreactivity (red in a–d), anti-acetylated α-tubulin immunoreactivity (glow in e, e′, f, and f′), and nuclear counterstain (cyan in a–f). Dorsal views; anterior is up in all images. Dotted lines in (a–d) indicate the outlines of each trunk ganglion. The images in (e′) and (f′) correspond to those in (e) and (f) but with the nuclear counterstain omitted. (a) The first trunk ganglion shows a diffuse but prominent synapsin signal in the middle region (arrowhead). (b) The second trunk ganglion shows a similar synapsin signal to the first trunk ganglion (arrowhead). (c) The third trunk ganglion is the only one with separate bilateral synapsin domains (arrowheads). (d) The fourth trunk ganglion is the only one where the synapsin signal is located in the anterior half of the ganglion (arrowhead). (e, e′, f, f′) Each of the trunk ganglia show a unique morphology, including the number and position of commissures (arrowheads). Interpedal commissures are present anterior to the trunk ganglia 2–4. aln, anterior leg nerve; con, connectives; inc, inner connectives; ipc, interpedal commissures; pln, posterior leg nerve; trg1–trg4, trunk ganglia 1–4. Scale bars: 5 μm (in all images)

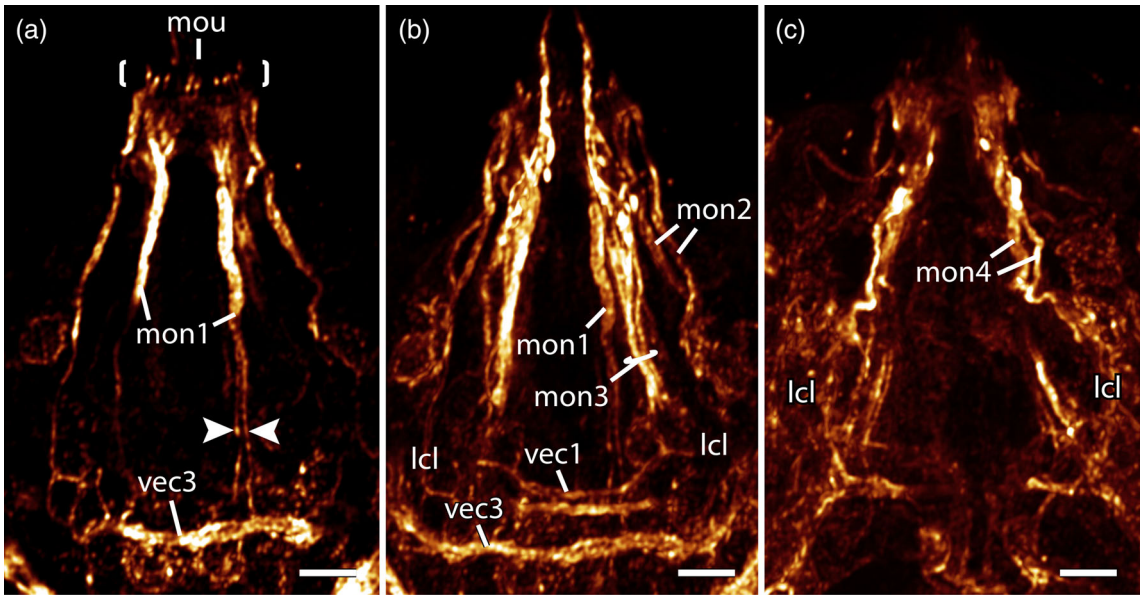

FIGURE 7 *Echiniscus testudo*, innervation of the mouth region. Maximum intensity projections of CLSM substacks showing anti-acetylated α-tubulin immunoreactivity. Dorsal views, anterior is up in all images. (a) Ventral region of the head showing the ventral-most double pair of mouth nerves (mouth nerves 1; arrowheads) that meet ventral commissure 3 on either side of the ventral midline. Notice how the neurites of the mouth nerves spread out distally to surround the mouth cone (brackets). (b) Substack showing a region immediately dorsal to that in (a), where mouth nerves 3 leave the ventrolateral clusters around their middle region, in close proximity to the ends of ventral commissure 1. Mouth nerves 2 leave the ventrolateral clusters at their anterior margin. (c) Substack showing the region immediately dorsal to that in (b), where mouth nerves 4 are located dorsal and slightly medial to mouth nerves 2. lcl, ventrolateral clusters; mon1–mon4, mouth nerves 1–4; mou, mouth opening; vec1, vec3, ventral commissures 1 and 3. Scale bars: 3 μm (in all images)

nerves are wide, showing a brush-like morphology that, all together, completely encircle the mouth opening (Figure 7a).

3.5 | Trunk ganglia

Each of the four segmental trunk ganglia in *E. testudo* exhibits a unique morphology when labeled against acetylated α-tubulin or synapsin (Figure 6a–f). Anti-acetylated α-tubulin immunolabeling reveals the prominent connectives linking each of the trunk ganglia to each other and linking the first trunk ganglion to the brain (Figures 1 and 6e,f). Each trunk ganglion additionally exhibits one pair of anterior and one pair of posterior leg nerves as well as a diffuse central fiber mass, that is, a meshwork of neurites with a number of distinguishable commissures that vary between ganglia (Figure 6e,f).

The first trunk ganglion is characterized by two pairs of connectives linking it to the central nervous system in the head as well as a single prominent commissure towards the posterior of the central fiber mass (Figure 6e). Anti-synapsin immunolabeling reveals a strong but diffuse signal spread throughout the central fiber mass (Figure 6a). The second trunk ganglion is the only ganglion with two distinguishable commissures: one at the anterior margin of the central fiber mass and one towards the posterior (Figure 6e). An interpedal commissure is present anterior to the second trunk ganglion but is not associated with any neuronal somata in its immediate vicinity, indicating that the interpedal commissures may simply be crossing points for contralateral commissures between ganglia (Figure 6e). Similar interpedal commissures are also found anterior to the third and fourth trunk ganglia (Figure 6e,f). Anti-synapsin immunolabeling shows a diffuse signal in the second trunk ganglion, weaker than that in the first ganglion but similarly spread across the central fiber mass (Figure 6b). The third trunk ganglion lacks any distinguishable commissures within the central fiber mass, reflected by a synapsin immunoreactivity that is restricted to the lateral regions where the connectives enter the ganglion (Figure 6c,e). Finally, the fourth trunk ganglion is narrower than the other three and possesses a single distinguishable commissure, located approximately in the middle of the central fiber mass (Figure 6f). The synapsin signal spans the width of the ganglion and, different from the other three ganglia, is concentrated around the position of the single commissure in the anterior half of the ganglion (Figure 6d).

4 | DISCUSSION

4.1 | Comparison to previous descriptions of the nervous system in representatives of Echiniscoidea

The most detailed description to date of the nervous system of an echiniscoidean heterotardigrade is that of Schulze and Schmidt-Rhaesa (2013), who also studied *E. testudo*. Although those authors used an antibody against tyrosinated α-tubulin (in addition to an

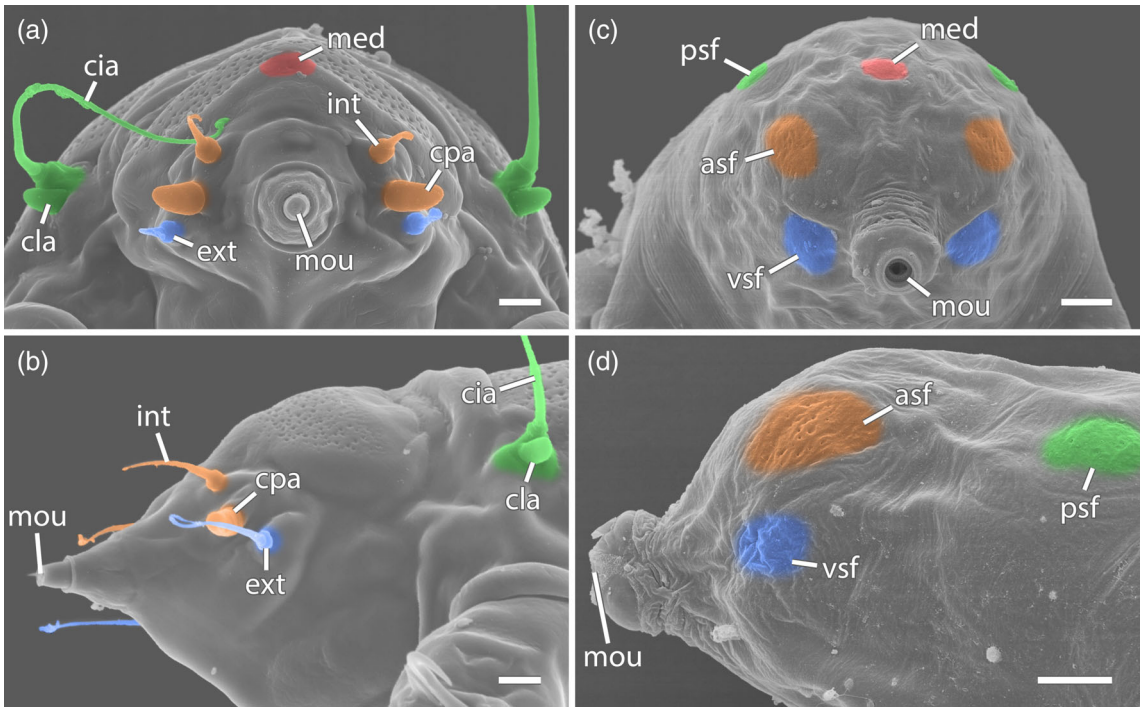

FIGURE 8 Hypothesis for the homology of cephalic sensory structures in heterotardigrades and eutardigrades. False-colored scanning electron micrographs of the heterotardigrade *Echiniscus testudo* (a, b) and the eutardigrade *Hypsibius exemplaris* (c, d) showing hypothetically homologous cephalic sensory structures based on innervation patterns (eutardigrade data based on Biserova & Kuznetsova, 2012; Mayer et al., 2013; Persson et al., 2012; Zantke et al., 2008; V. Gross, unpublished data). Frontal (a, c) and lateral (b, d) views. Anterior is left in (b, d); dorsal is up in all images. Cephalic sensory fields of *H. exemplaris* are recognizable externally by the presence of pores or a locally modified appearance of the cuticle. Note that neurites of the internal cirrus and cephalic papilla together may correspond to the anterolateral sensory field and the clava and cirrus A together may correspond to the posteriolateral sensory field. asf, anterolateral sensory field; cia, cirrus A; cla, clava; cpa, cephalic papilla; ext, external cirrus; int, internal cirrus; med, median sensory field; mou, mouth; psf, posterolateral sensory field; vsf, ventrolateral sensory field. Scale bars: 5 μm (in all images)

antibody against RFamide), our results based on acetylated α-tubulin immunoreactivity generally reflect their findings. While we do refer to distinct regions when describing the brain, we decided to avoid wherever possible the term "cluster" to describe apparent accumulations of neuronal somata—with the exception of the ventrolateral, ventral, and outer clusters—since our data indicate that the apparent morphology of these can vary considerably depending on the position of the animal and the degree of deformation introduced during specimen preparation. As such, the "anterior," "dorsal," and "inner clusters" described by Schulze and Schmidt-Rhaesa (2013) all fall within our definition of the brain (Table 1). On the other hand, we label the "posterior clusters" described by Schulze and Schmidt-Rhaesa (2013) as "outer clusters," since they are unmistakably spatially separated from the brain, not only in the posterior but also in the lateral direction. For the regions referred to by Schulze and Schmidt-Rhaesa (2013) as "dorsoventral clusters" ("neurite clusters" *sensu* Smith et al., 2017), we introduce the term "ventrolateral clusters" to more precisely describe their position in *E. testudo* and to emphasize the distinction between this region and the dorsal brain.

It should be noted that in their description of the brain of the related species *Viridiscus viridissimus* (Peterfi, 1956), Dewel and Dewel (1996) refer to a number of ganglia and neuropils innervating the cephalic sensilla in the head. These structures correspond to at least a subset of the clusters and commissures described herein and by Schulze and Schmidt-Rhaesa (2013) for *E. testudo*, but their identities as ganglia (*sensu* Richter et al., 2010) and neuropils ("synapsin-rich neuropils" *sensu* Ito et al., 2014) are not supported by immunohistochemical data.

4.2 | Implications for the organization of the tardigrade brain

The nature of the ventrolateral clusters, and more generally the ventral nervous system in the head, has been a topic of extensive discussion in the past, specifically whether these regions might represent distinct, segmental lobes of the brain (e.g., Persson et al., 2012; Persson et al., 2014) or reflect a circumpharyngeal organization of the brain (Marcus, 1929). Our data do not support a circumpharyngeal brain in tardigrades as is typical of the non-panarthropod ecdysozoans (also known as cycloneuralians) for two reasons. First, there is no evidence for an anterior-to-posterior perikarya-neuropil-perikarya organization of the brain (Schmidt-Rhaesa & Henne, 2016). Second, the neuropil region in the head does not form a ring but is instead

TABLE 1 Summary of the terminology of neural (sub)structures in the head of *Echiniscus testudo*

This study	Schulze and Schmidt-Rhaesa (2013)
Brain (brn)	
—	Dorsal cluster (dcl)
—	Inner cluster (icl)
—	Anterior cluster (acl)
Cerebral tracts	
Brain commissure 1 (brc1)	Dorsal commissure 2 (dcm2)
Brain commissure 2 (brc2)	Dorsal commissure 3 (dcm3)
Fork of brain commissure 2 (foc)	Dorsal commissure 1 (dcm1)
Posterior nerve tract (pnt)	—
Inner connectives (inc)	Inner connectives (cn_i)
Outer connectives (ouc)	Outer connectives (cn_o)
Neurite bridge between brain and outer cluster (obr)	Dorsal neurite (dn_{pcl})
Extracerebral commissures	
Stomodeal commissure 1 (stc1)	Dorsal commissure 5 (dcm5)
Stomodeal commissure 2 (stc2)	Dorsal commissure 6 (dcm6)
Stomodeal commissure 3 (stc3)	Dorsal commissure 4 (dcm4)
Ventral commissure 1 (vec1)	Third ventral commissure (vcm3)
Ventral commissure 2 (vec2)	Second ventral commissure (vcm2)
Ventral commissure 3 (vec3)	First ventral commissure (vcm1)
Extracerebral cell clusters	
Outer cluster (ocl)	Posterior cluster (pcl)
Ventrolateral cluster (lcl)	Dorsoventral cluster (dvcl)
Ventral cluster (vcl)	Ventral cluster (vcl)
Neurites associated with cephalic sensory structures	
Neurites of internal cirrus (icn)	Dorsal neurite (dn_{ic})
Neurites of external cirrus (ecn)	Dorsal neurite (dn_{ec})
Neurites of median cirrus (mcn)	Dorsal neurite (dn_m)
Neurites of clava (cvn)	Dorsal neurite (dn_{pcl})
Neurites of cirrus A (can)	Dorsal neurite (dn_{pcl})
Neurites of cephalic papilla (cpn)	Dorsal neurite (dn_{cp})
Mouth nerves 1–4 (mon1–mon4)	—
Central nervous system in the trunk	
Trunk ganglia 1–4 (trg1–trg4)	Ventral ganglia 1–4 (gI–gIV)
Anterior leg nerve (aln)	Neurites 1 and 2 (n_1, n_2)
Posterior leg nerve (pln)	Neurite 3 (n_3)
Interpedal commissure (ipc)	Ganglion independent commissure
Connectives (con)	Connectives (cn)

Note: Abbreviations used in the figures are provided in parentheses after each term. For comparison, terminology from Schulze and Schmidt-Rhaesa (2013) is also included.

restricted to the dorsal and dorsolateral space in *E. testudo*. Similarly, synapsin signal was also found exclusively within the dorsally located central brain neuropil in the arthrotardigrade *Actinarctus doryphorus ocellatus* (Schulze et al., 2014).

Unfortunately, to our knowledge, no synapsin labeling data are available from cycloneuralians to compare, but we anticipate the synapsin signal to be present throughout the ring-shaped neuropil (*sensu* Ito et al., 2014) in representative species, as ultrastructural studies revealed synapses in this structure (Rehkämper et al., 1989; Ware et al., 1975). By contrast, if synapsin is in fact found to be restricted to the dorsal region of the brain, the nature and organization of the entire cycloneuralian brain, as well as the evolutionary implications thereof, would need to be reevaluated. In such a case, the tardigrade central nervous system would bear a much closer resemblance to the cycloneuralian nervous system than to that of the other panarthropods (Gross & Mayer, 2015; Martin et al., 2017), providing

morphological support and strengthening the case for a close tardigrade-cycloneuralian relationship (Yoshida et al., 2017). To date, however, there is no morphological evidence suggesting this may be the case.

While we can conclude that the brain neuropil is serially homologous to the neuropil of each ganglion, one must bear in mind that the synapsin signal is unique in each of the four trunk ganglia and the head. The synapsin signal in the ganglia does not always correspond to the distinct commissures revealed by anti-acetylated α-tubulin immunolabeling. We therefore urge caution when using commissure similarity as the only evidence for homologizing brain lobes and trunk ganglia (see also "tripartite hypothesis II" in Smith & Goldstein, 2017). At the same time, we cannot exclude the possibility that part of the ventrolateral cluster may correspond to parts of the trunk ganglion, as previously suggested by Smith et al. (2017). In this scenario, the ventrolateral clusters may be serially homologous to regions of the ganglia containing somata and synapsin-free neurites. Additional experiments with the goal of localizing potentially serially homologous cells by using neuronal markers such as serotonin or dopamine (Brenneis & Scholtz, 2015; Martin et al., 2017), for example, may be more informative in terms of testing this hypothesis in *E. testudo*. Anti-synapsin immunolabeling in the non-panarthropod ecdysozoans would also go a long way in helping to reconstruct the ancestral pattern of synapsin distribution in the brains of panarthropods and ecdysozoans and aid in determining which brain regions are homologous.

4.3 | Homology of cephalic sensilla and sensory fields across tardigrades

Most morphological data to date from the cephalic sensory structures of various species show similar innervation patterns, whether based on ultrastructure (Biserova & Kuznetsova, 2012; Dewel et al., 1993; Wiederhöft & Greven, 1999) or immunohistochemistry (Schulze et al., 2014; Schulze & Schmidt-Rhaesa, 2013; Zantke et al., 2008), suggesting homology between the cephalic sensilla of heterotardigrades and the sensory fields of eutardigrades (Figure 8). The innervation pattern of the cephalic sensilla of *E. testudo* revealed by our immunohistochemical data also largely mirror those of the sensory fields of eutardigrades, for example, those of *Mesobiotus* cf. *harmsworthi* (Mayer et al., 2013), *Halobiotus crispae* (Persson et al., 2012), *Halobiotus stenostomus* (Biserova & Kuznetsova, 2012), and *Macrobiotus hufelandi* (Zantke et al., 2008). Similarly, we also found innervation of a putative median cirrus homolog in *E. testudo*, although the external morphology of this region more closely resembles a sensory field than a sensillum (i.e., lack of a prominent sensory structure but presence of a pore in the cuticle).

Biserova and Kuznetsova (2012) noted that the somata of the neurons innervating the lateral sensory fields in *H. stenostomus* are located within the brain (i.e., deeper inside the head) while those innervating the cirri in the arthrotardigrade *Halechiniscus greveni* are located directly under their respective structures (Kristensen, 1981). While this pattern is reflected in our data, where neurons of the outer cluster lie underneath and innervate the clava and cirrus A, we stress that the outer cluster maintains a direct connection to the central brain neuropil. In our view, innervation patterns and interconnections between neurons are more meaningful in an evolutionary sense than the absolute positions of neuronal somata. We, therefore, do not consider the difference in the positions of these somata between heterotardigrades and eutardigrades as an argument against the homology of the sensilla and sensory fields, but rather a product of the general shape of the head and the shape and position of the brain within it. While additional differences have also been documented, for example, the clavae of heterotardigrades possess microvilli while eutardigrade sensory fields do not, for example (Biserova & Kuznetsova, 2012; Kristensen, 1981), our data as well as those of previous studies support the prevailing hypothesis that at least a subset of the cephalic sensilla of heterotardigrades is homologous with the sensory fields of eutardigrades.

Based on a comparison of our data with the literature (Biserova & Kuznetsova, 2012; Mayer et al., 2013; Persson et al., 2012; Zantke et al., 2008), we propose that (a) the cirrus A and clava together are homologous to the posterolateral sensory field, (b) the internal cirrus and cephalic papilla together are homologous to the anterolateral sensory field, (c) the external cirrus is homologous to the ventrolateral sensory field, and (d) the median sensory field of *E. testudo* (but probably also present in all echiniscoideans) is homologous to the median sensory field of eutardigrades. It should be noted that while Zantke et al. (2008) grouped the external cirrus and cephalic papilla together in their homology hypothesis, our data suggest that innervation of the cephalic papilla is instead more closely associated with that of the internal cirrus, with the neurites of the external cirrus spatially separated from these structures and the brain. Future immunohistochemical studies on the apochelan eutardigrade *Milnesium tardigradum*, which exhibits sensory fields in addition to a pair of cephalic papillae, may help clarify putative homologies of the cephalic sensory structures between heterotardigrades and eutardigrades.

5 | CONCLUSIONS

The anti-synapsin immunolabeling presented herein shows that there is still much to learn about the tardigrade brain and its different regions. While neuropils may also be identifiable using transmission electron microscopy (Dewel & Dewel, 1996), immunohistochemistry allows for the co-localization of specific cell types (Schulze et al., 2014). Whether the different lobes or subregions of the tardigrade brain are specialized for any particular function may be elucidated with such experiments in the future, while comparative studies with other taxa may provide further insights into the evolution of the tardigrade brain and central nervous system in general. Individually identifiable neurons have previously been used as landmarks to homologize substructures in related taxa (Brenneis & Scholtz, 2015), and there is no reason to believe that the same should not be possible in tardigrades.

ACKNOWLEDGMENTS

The authors thank Łukasz Michalczyk (Jagiellonian University, Kraków) for his help with identifying the species and Sarah Atherton (Swedish Museum of Natural History) for proofreading the manuscript. The authors further thank two anonymous reviewers, whose comments helped to improve the manuscript.

CONFLICT OF INTEREST

The authors declare that they have no conflict of interest.

AUTHOR CONTRIBUTIONS

Vladimir Gross: Conceptualization; investigation; methodology; visualization; writing-original draft; writing-review & editing. **Lisa Epple:** Conceptualization; investigation; methodology; visualization; writing-original draft; writing-review & editing. **Georg Mayer:** Conceptualization; supervision; writing-review & editing.

PEER REVIEW

The peer review history for this article is available at https://publons.com/publon/10.1002/jmor.21386.

DATA AVAILABILITY STATEMENT

The data that support the findings of this study are available from the corresponding author upon reasonable request.

ORCID

Vladimir Gross https://orcid.org/0000-0001-7422-9148

Georg Mayer https://orcid.org/0000-0003-0737-2440

REFERENCES

Biserova, N. M., & Kuznetsova, K. G. (2012). Head sensory organs of *Halobiotus stenostomus* (Eutardigrada, Hypsibiidae). *Biology Bulletin*, *39*, 579–589. https://doi.org/10.1134/S1062359012070035

Brenneis, G., & Scholtz, G. (2015). Serotonin-immunoreactivity in the ventral nerve cord of Pycnogonida — Support for individually identifiable neurons as ancestral feature of the arthropod nervous system. *BMC Evolutionary Biology*, *15*, 136. https://doi.org/10.1186/s12862-015-0422-1

Dewel, R. A., & Dewel, W. C. (1996). The brain of *Echiniscus viridissimus* Peterfi, 1956 (Heterotardigrada): A key to understanding the phylogenetic position of tardigrades and the evolution of the arthropod head. *Zoological Journal of the Linnean Society*, *116*, 35–49.

Dewel, R. A., Nelson, D. R., & Dewel, W. C. (1993). Tardigrada. In F. W. Harrison & M. E. Rice (Eds.), *Microscopic anatomy of invertebrates* (Vol. 12, pp. 143–183). Wiley-Liss.

Gąsiorek, P., Stec, D., Morek, W., & Michalczyk, Ł. (2017). An integrative redescription of *Echiniscus testudo* (Doyère, 1840), the nominal taxon for the class Heterotardigrada (Ecdysozoa: Panarthropoda: Tardigrada). *Zoologischer Anzeiger*, *270*, 107–122. https://doi.org/10.1016/j.jcz.2017.09.006

Gross, V., & Mayer, G. (2015). Neural development in the tardigrade *Hypsibius dujardini* based on anti-acetylated α-tubulin immunolabeling. *EvoDevo*, *6*, 12. https://doi.org/10.1186/s13227-015-0008-4

Gross, V., & Mayer, G. (2019). Cellular morphology of leg musculature in the water bear *Hypsibius exemplaris* (Tardigrada) unravels serial homologies. *Royal Society Open Science*, *6*, 191159. https://doi.org/10.1098/rsos.191159

Ito, K., Shinomiya, K., Ito, M., Armstrong, J. D., Boyan, G., Hartenstein, V., Harzsch, S., Harzsch, S., Heisenberg, M., Homberg, U., Jenett, A., Keshishian, H., Restifo, L. L., Rössler, W., Simpson, J. H., Strausfeld, N. J., & Strauss, R. (2014). A systematic nomenclature for the insect brain. *Neuron*, *81*, 755–765. https://doi.org/10.1016/j.neuron.2013.12.017

Klagges, B. R. E., Heimbeck, G., Godenschwege, T. A., Hofbauer, A., Pflugfelder, G. O., Reifegerste, R., Reisch, D., Schaupp, M., Buchner, S., & Buchner, E. (1996). Invertebrate synapsins: A single gene codes for several isoforms in *Drosophila*. *The Journal of Neuroscience*, *16*, 3154–3165.

Kristensen, R. M. (1981). Sense organs of two marine arthrotardigrades (Heterotardigrada, Tardigrada). *Acta Zoologica*, *62*, 27–41.

Marcus, E. (1929). Tardigrada. In H. G. Bronn (Ed.), *Klassen und Ordnungen des Tier-Reichs wissenschaftlich dargestellt in Wort und Bild* (Vol. 5, pp. 1–609). Akademische Verlagsgesellschaft.

Martin, C., Gross, V., Hering, L., Tepper, B., Jahn, H., de Sena Oliveira, I., Stevenson, P. A., & Mayer, G. (2017). The nervous and visual systems of onychophorans and tardigrades: Learning about arthropod evolution from their closest relatives. *Journal of Comparative Physiology A*, *203*, 565–590. https://doi.org/10.1007/s00359-017-1186-4

Martin, C., Gross, V., Pflüger, H.-J., Stevenson, P. A., & Mayer, G. (2017). Assessing segmental versus non-segmental features in the ventral nervous system of onychophorans (velvet worms). *BMC Evolutionary Biology*, *17*, 3. https://doi.org/10.1186/s12862-016-0853-3

Mayer, G., Kauschke, S., Rüdiger, J., & Stevenson, P. A. (2013). Neural markers reveal a one-segmented head in tardigrades (water bears). *PLoS One*, *8*, e59090. https://doi.org/10.1371/journal.pone.0059090

Neumann, M., & Gabel, D. (2002). Simple method for reduction of autofluorescence in fluorescence microscopy. *The Journal of Histochemistry and Cytochemistry*, *50*, 437–439. https://doi.org/10.1177/002215540205000315

Ott, S. R. (2008). Confocal microscopy in large insect brains: Zinc-formaldehyde fixation improves synapsin immunostaining and preservation of morphology in whole-mounts. *Journal of Neuroscience Methods*, *172*, 220–230. https://doi.org/10.1016/j.jneumeth.2008.04.031

Persson, D. K., Halberg, K. A., Jørgensen, A., Møbjerg, N., & Kristensen, R. M. (2012). Neuroanatomy of *Halobiotus crispae* (Eutardigrada: Hypsibiidae): Tardigrade brain structure supports the clade Panarthropoda. *Journal of Morphology*, *273*, 1227–1245. https://doi.org/10.1002/jmor.20054

Persson, D. K., Halberg, K. A., Jørgensen, A., Møbjerg, N., & Kristensen, R. M. (2014). Brain anatomy of the marine tardigrade *Actinarctus doryphorus* (Arthrotardigrada). *Journal of Morphology*, *275*, 173–190. https://doi.org/10.1002/jmor.20207

Rehkämper, G., Storch, V., Alberti, G., & Welsch, U. (1989). On the fine structure of the nervous system of *Tubiluchus philippinensis* (Tubiluchidae, Priapulida). *Acta Zoologica (Stockholm)*, *70*, 111–120.

Richter, S., Loesel, R., Purschke, G., Schmidt-Rhaesa, A., Scholtz, G., Stach, T., Vogt, L., Wanninger, A., Brenneis, G., Döring, C., Faller, S., Fritsch, M., Grobe, P., Heuer, C. M., Kaul, S., Møller, O. S., Müller, C. H. G., Rieger, V., Rothe, B. H., … Harzsch, S. (2010). Invertebrate neurophylogeny: Suggested terms and definitions for a neuroanatomical glossary. *Frontiers in Zoology*, *7*, 29. https://doi.org/10.1186/1742-9994-7-29

Rueden, C. T., Schindelin, J., Hiner, M. C., DeZonia, B. E., Walter, A. E., Arena, E. T., & Eliceiri, K. W. (2017). ImageJ2: ImageJ for the next generation of scientific image data. *BMC Bioinformatics*, *18*, 529. https://doi.org/10.1186/s12859-017-1934-z

Schmidt-Rhaesa, A., & Henne, S. (2016). Cycloneuralia (Nematoda, Nematomorpha, Priapulida, Kinorhyncha, Loricifera). In A. Schmidt-Rhaesa, S. Harzsch, & G. Purschke (Eds.), *Structure and evolution of invertebrate nervous systems* (pp. 368–381). Oxford University Press.

Schulze, C., Neves, R. C., & Schmidt-Rhaesa, A. (2014). Comparative immunohistochemical investigation on the nervous system of two species of Arthrotardigrada (Heterotardigrada, Tardigrada). *Zoologischer Anzeiger*, *253*, 225–235. https://doi.org/10.1016/j.jcz.2013.11.001

Schulze, C., & Schmidt-Rhaesa, A. (2013). The architecture of the nervous system of *Echiniscus testudo* (Echiniscoidea, Heterotardigrada). *Journal of Limnology*, *72*, 44–53. https://doi.org/10.4081/jlimnol.2013.s1.e6

Smith, F. W., Bartels, P. J., & Goldstein, B. (2017). A hypothesis for the composition of the tardigrade brain and its implications for the panarthropod brain evolution. *Integrative and Comparative Biology*, *57*, 546–559. https://doi.org/10.1093/icb/icx081

Smith, F. W., Boothby, T. C., Giovannini, I., Rebecchi, L., Jockusch, E. L., & Goldstein, B. (2016). The compact body plan of tardigrades evolved by the loss of a large body region. *Current Biology*, *26*, 224–229. https://doi.org/10.1016/j.cub.2015.11.059

Smith, F. W., Cumming, M., & Goldstein, B. (2018). Analyses of nervous system patterning genes in the tardigrade *Hypsibius exemplaris* illuminate the evolution of panarthropod brains. *EvoDevo*, *9*, 19. https://doi.org/10.1186/s13227-018-0106-1

Smith, F. W., & Goldstein, B. (2017). Segmentation in Tardigrada and diversification of segmental patterns in Panarthropoda. *Arthropod Structure & Development*, *46*, 328–340. https://doi.org/10.1016/j.asd.2016.10.005

Telford, M. J., Pisani, D., & Rota-Stabelli, O. (2019). Phylo-evo-devo, tardigrades and insights into the evolution of segmentation. In G. Fusco (Ed.), *Perspectives on evolutionary and developmental biology* (pp. 191–199). Padova University Press.

Ware, R. W., Clark, D., Crossland, K., & Russel, R. L. (1975). The nerve ring of the nematode *Caenorhabditis elegans*: Sensory input and motor output. *Journal of Comparative Neurology*, *162*, 71–110.

Wiederhöft, H., & Greven, H. (1999). Notes on head sensory organs of *Milnesium tardigradum* Doyère, 1840 (Apochela, Eutardigrada). *Zoologischer Anzeiger*, *238*, 338–346.

Yoshida, Y., Koutsovoulos, G., Laetsch, D. R., Stevens, L., Kumar, S., Horikawa, D. D., Ishino, K., Komine, S., Kunieda, T., Tomita, M., Blaxter, M., & Arakawa, K. (2017). Comparative genomics of the tardigrades *Hypsibius dujardini* and *Ramazzottius varieornatus*. *PLoS Biology*, *15*, e2002266. https://doi.org/10.1371/journal.pbio.2002266

Zantke, J., Wolff, C., & Scholtz, G. (2008). Three-dimensional reconstruction of the central nervous system of *Macrobiotus hufelandi* (Eutardigrada, Parachela): Implications for the phylogenetic position of Tardigrada. *Zoomorphology*, *127*, 21–36. https://doi.org/10.1007/s00435-007-0045-1

SUPPORTING INFORMATION

Additional supporting information may be found online in the Supporting Information section at the end of this article.

How to cite this article: Gross, V., Epple, L., & Mayer, G. (2021). Organization of the central nervous system and innervation of cephalic sensory structures in the water bear *Echiniscus testudo* (Tardigrada: Heterotardigrada) revisited. *Journal of Morphology*, *282*(9), 1298–1312. https://doi.org/10.1002/jmor.21386